ISSN 2345 - 4997

Available online at: www.geo-dynamica.com

Vol. (I) - No. 02- (Special Issue on Intra- Plate Earthquakes) Feb.2014
1st Article- P. 1 to 14

GRIB
Geodynamics Research International Bulletin

Determination of Moho Discontinuity from Satellite Gradiometry Data: A Linear Approach

Mehdi Eshagh

Department of Engineering Science, University West, Trollhättan, Sweden.

mehdi.eshagh@hv.se

Article History:	Received: Jan. 16, 2014	Reviewed: Jan. 19, 2014
Revised: Jan. 22, 2014	Accepted: Feb. 05, 2014	Published: Feb. 14, 2014

ABSTRACT

The satellite gradiometry data (SGD) can be used for studying the crustal structure in addition to the Earth's gravity field. This paper will show how this type of data is related to the Moho discontinuity or the boundary between the Earth's crust and mantle. Here, the Vening Meinesz-Moritz (VMM) theory of isostasy is used and its mathematical formulae are modified to use the SGD instead of the Earth gravity models. A linear integral equation with a well-behaving kernel is presented by approximating the Moho depth formula derived based on the VMM theory. The error of this approximation is less than 300 m in Iran as the study area. Furthermore, this paper shows that the contribution of the higher degree harmonics than 215 is less than 1% with respect to the total signal of Moho undulations. This means that the use of SGD is meaningful as they sense the harmonics of the Earth's gravity field to this degree. Two methods of one-step and two-step are proposed for Moho determination and applied in Iran. It is shown that to reduce the effect of spatial truncation error of the integral formulae of both methods the central area should be smaller by 6° than the inversion area. Numerical studies show that the two-step approach is superior to the other one and the root mean squared error of differences between the Moho model recovered by an Earth gravity model and SGD is about 1.5 km in Iran.

Keywords: Inversion, Satellite Gradiometer, Topographic Masses, Iran, Regularisation.

1. INTRODUCTION

The gravity field and steady-state ocean circulation explorer (GOCE) is dedicated to recover a precise high resolution gravity field for the Earth. In this satellite mission the differential accelerometry technique is used to measure the gravity gradients in a gradiometer mounted in the spacecraft. This technique is called satellite gravity gradiometry. This mission is expected to deliver gravity models to degree and order 250. The satellite gradiometry data (SGD) can be used to recover regional gravity field directly (see e.g. Reed 1973, Xu 1992, 1998, 2009, Janak et al. 2009 and Eshagh 2009a, Eshagh and Sjöberg 2011). Studying the interior structure of the Earth is also possible using the SGD data but the main issue is to find the proper mathematical relations between the data and the interior quantities. The Moho surface is the boundary between the Earth's crust and mantle and either the seismic or gravimetric data can be used for determining this surface. The seismic Moho surface is the interface at which a seismic wave velocity jump occurs and the gravimetric one is the surface obtained from inversion of gravimetric data by assuming a density contrast at the crust-mantle transition according to isostatsy. The isostatic hypothesis comes from the fact that the crust is floating on the viscose mantle and its principle states that the crust is thicker under mountainous areas than in flat areas due to the lack of mass beneath the mountains chain. Airy (1855) stated that the isostatic compensation is locally achieved by variation in the thickness of the crust and Vening Meinesz (1931) modified it to regional compensation. Heiskanen (1931) presented a method to estimate the crustal thickness by considering a regional instead of local compensation of topographic masses. Parker (1972) presented a practical iterative gravimetric method based on a constant density contrast and a varying Moho depth, similar to Vening Meinesz's hypothesis, in the Fourier domain and planar approximation. Due to the instability of this method Oldenburg (1974) added a filter in the frequency domain to stabilise the solution. Combination of these two methods was generalised to three dimensions by Gomes-Ortiz and Agarwal (2005) and Shin et al. (2007). Kiamehr and Gomes-Ortiz (2009) applied this three dimensional method and estimated the Moho depth in Iran based on the terrestrial gravimetric data and the Earth gravity model EGM08 (Pavlis et al. 2008). Čadak and Martinec (1991) presented the first global model of Moho in terms of the spherical harmonics to degree and order 30 based on different sources of

seismic data. Martinec (1993 and 1994) studied the determination of the density contrast between the mantle and crust by minimising the sum of the squares of the gravitational potentials induced by the Earth's topographic masses and Moho. Sünkel (1985) converted the Airy-Heiskanen Moho depth to the Vening Meinesz by smoothing it further so that the global mean squared error of difference between disturbing and topographic-isostatic potentials is minimised. Sjöberg and Bagherbandi (2011) presented a method for the estimation of the density contrast using EGM08 and CRUST2.0 and Tenzer et al. (2012) similarly studied this issue by including the ice model, ICE-5G. Eshagh (2009b, 2010) studied the effect of lateral density variation in the crustal and topographic masses on the SGD.

The current lack of knowledge about the density structure within the Earth's crust is a major limiting factor of estimating the Moho density interface accurately. The crustal density contrast stripping corrections were applied systematically to the topographically-corrected gravity field using CRUST2.0 in Tenzer et al. (2009). Moritz (1990) improved the Vening Meinesz hypothesis by developing it to a spherical Earth model with some approximations which were not suitable for inverting the gravity data. Sjöberg (2009) reformulated this problem in a more proper way and presented a new solution for the theory of Moritz, named it the Vening Meinesz-Moritz (VMM) inverse problem in isostasy. He presented some iterative as well as approximate spherical harmonic solutions. Bagherbandi and Sjöberg (2011) compared the gravimetric local Airy-Heiskanen and the VMM models with the seismic CRUST2.0 global model (Bassin et al. 2000) for estimating the Moho depth. They found that the VMM model is consistent with the Moho model of CRUST2.0 with a global uncertainty of 7 km. Braitenberg et al. (2000) presented an iterative inversion method to obtain the variation of Moho in the Tibet plateau. Their investigation shows that the results of the gravity inversion for the Moho recovery and the seismic Moho model have an uncertainty of about ±5 km. This tolerance is because of disregarding dynamic effects involved in Tibet such as uplift is underlying of Tibet by the Indian plate. In another study, Braitenberg et al. (2006) formulated a crustal model of South China Sea by constrained forward and inverse gravity modelling from the combined analysis of models of satellite gravity field, bathymetric, sediment and crustal thicknesses and the isostatic flexure. They considered the effect of the sediment layer using the global sediment thickness model of NOAA (National Oceanic and Atmospheric Administration) and fitted the sediment compaction model to observed crustal density values. Sampietro (2009) studied the problem of recovering the Moho depth from the GOCE data in a simulation study and found that the Moho model can be recovered from SGD with an accuracy of about 2 km. Braitenberg and Ebbing (2009) used GRACE (Gravity Recovery and Climate Experiment) satellite data (Tapley et al. 2005) and terrestrial gravity data to study the structure of the crust. They presented a three-dimensional method based on forward modelling which uses a priori known crustal structures. The gravity data of the study area is estimated using this method and compared to the observed ones. Their residuals were used for identification of density anomalies not previously recognised. The idea of combining the seismic and gravimetric models of Moho presented by Eshagh et al. (2011) using their spherical harmonics and later on Eshagh and Bagherbandi (2012) combined these two models locally in Fennoscandia and estimated the qualities of the models.

In Shin et al. (2007) a recovery of the Moho depth from satellite data was performed. They presented an updated model of the Moho undulations on an extended area using an improved gravity data set, which at long wavelengths relies entirely on the new results of the GRACE mission. They tried to invert the gravity anomalies using the Parker-Oldenburg method (Oldenburg 1974). Sampietro (2011) considered the local inversion of the SGD by simulating a Moho surface and generating the SGD from them. However, some planar approximations were used in his formulation and the problem of spatial truncation error (STE) of the integral formulae and the behaviour of their kernels was not considered. Sampietro and Reguzzoni (2011) implemented a method based on collocation and fast Fourier transform to evaluate the GOCE data in the Moho estimation. They considered the STE by applying a larger region than the study area. Reguzzoni and Sampietro (2012) presented a global crustal model based on the GOCE data and Reguzzoni et al. (2013) combined the seismic model of CRUST2.0 and the one derived from GOCE and presented a new combined Moho model. Barzaghi et al. (2013) presented a collocation-based method for combining the global Moho model derived from GOCE and the local one by terrestrial data.

Bagherbandi and Eshagh (2011 and 2012) investigated this issue by reformulating the VMM theory according to the second-order derivative of the disturbing potential instead of the gravity anomaly and Earth gravity models. They obtained a nonlinear integral equation and solved it iteratively using Tikhonov Regularisation (Tikhonov 1963). The main idea of this paper is to perform a similar study but with a simpler linear method to avoid any iteration in the solution. Sjöberg (2009) presented a mathematical formula for Moho model which has three terms which are functions of an approximate Moho model. Therefore, if we can estimate this

approximate model from other type of data, therefore, the generation of the second and third terms will not be difficult. Recovering this approximate Moho model from the SGD is a novel idea and we further investigate the approximation error of our method and the highest meaningful degree of the spherical harmonic expansion of the Moho model. Two methods for Moho recovery are presented and both of them are applied in Iran.

2. MATERIALS AND METHODS

2. 1. MATHAMATICAL MODELS OF OBSERVABLES AND MOHO DEPTHS

The disturbing potential outside the Earth's surface is expressed by the following spherical harmonic expansion (Heiskanen and Moritz 1967, p. 35):

$$V=\sum_{n=2}^{\infty}\left(\frac{R}{r}\right)^{n+1}\sum_{m=-n}^{n}v_{nm}Y_{nm}(\theta,\lambda),\quad r>R \tag{1}$$

where R is the semi-major axis of the reference ellipsoid, r the geocentric distance of the computation point, v_{nm} is the spherical harmonic coefficient of degree n and order m of the disturbing potential and $Y_{nm}(\theta,\lambda)$ stands for the fully-normalised spherical harmonics at the co-latitude θ and longitude λ. Since we assume that the normal gravity field has the same mass as that of the Earth and the coordinate system is geocentric we do not consider the zero- and first-degree harmonics in the series (1). The second-order radial derivative of the disturbing potential is derived by taking the derivative of Eq. (1) twice with respect to r (cf. Martinec 2003):

$$V_{rr}=\frac{1}{R^2}\sum_{n=2}^{\infty}(n+1)(n+2)\left(\frac{R}{r}\right)^{n+3}\sum_{m=-n}^{n}v_{nm}Y_{nm}(\theta,\lambda). \tag{2}$$

Equation (2) is the mathematical formula of our observables and our goal is to find its relation to its Moho depths formula. Now, we present the mathematical formula of the Moho depth presented by Sjöberg (2009) according to the VMM theory:

$$T_{\text{Moho}}=T+\frac{T^2}{R}-\frac{1}{8R}\iint_{\sigma}\frac{T'^2-T^2}{\sin^3(\psi/2)}d\sigma \tag{3}$$

where σ is the unit sphere and $d\sigma$ the surface integration element and ψ stands for the geocentric angle between the computation point and integration points. Note that in Eq. (3) the integration point is shown by prime. Furthermore, the approximate Moho depth has the following spectral form:

$$T=\sum_{n=0}^{\infty}T_n \tag{4}$$

where

$$T_n=-\frac{A_{C0}}{4\pi k}\delta_{n0}+2\pi\nu_n(\mu H)_n-\nu_n\Delta g_n \tag{5}$$

and δ stands for Kronecker's delta, $k=G\Delta\rho$ and G is the Newtonian gravitational constant and $\Delta\rho$ the density contrast between the crust and mantle, H the topographic information of the solid Earth surface and μ the density of crust. A_{C0} is named the normal compensation attraction with the following formula (Sjöberg 2009):

$$A_{C0}=\frac{4\pi kR}{3}\left[\left(1-\frac{T_0}{R}\right)^3-1\right] \tag{6}$$

and finally

$$\nu_n=\frac{1}{4\pi k}\frac{2n+1}{n+1} \tag{7}$$

$$(\mu H)_n=\sum_{m=-n}^{n}\frac{1}{4\pi}\iint_{\sigma}(\mu H)Y_{nm}(\theta',\lambda')d\sigma Y_{nm}(\theta,\lambda) \tag{8}$$

$$\mu H=\begin{cases}\mu H & \text{if } H\geq 0\\ (\mu_w-\mu)H & \text{if } H<0\end{cases} \tag{9}$$

where μ_w is density of water.

By looking at Eq. (3), which is the formula for computing the Moho depth, we observe that T should be computed first and after that two correcting terms are added to improve T. This equation does not involve any other information and T plays the main role for computing the Moho depth. On the other hand, the contribution of the integral term of Eq. (3) is not very significant and in order of metres which is negligible and once T is computed, the computation of the second term of Eq. (3) is very straightforward. Here, we name the second term in the right hand side (r.h.s) of Eq. (5) the Bouguer contribution to the Moho depth.

2.2. ONE-STEP APPROACH

The Moho depth, which is presented by Eq. (3), requires the Laplace harmonics of the gravity anomaly at sea level. Such an anomaly has the following relation with the spherical harmonic coefficients of the disturbing potential (Heiskanen and Moritz 1967, p. 97):

(10) $$\Delta g_n = \frac{n-1}{R}\sum_{m=-n}^{n} v_{nm} Y_{nm}(\theta,\lambda).$$

By comparing Eq. (10) and Eq. (2) the following relation between the Laplace harmonic of the gravity anomaly and that of the SGD is derived:

(11) $$\Delta g_n = \frac{r^2}{R} w_n V_{rr,n} \text{ where } w_n = \frac{(n-1)}{(n+1)(n+2)}\left(\frac{r}{R}\right)^{n+1}.$$

Substitution of Eq. (11) into Eq. (5) and further simplification of the result reads:

(12) $$\frac{R}{r^2}\sum_{n=2}^{\infty}\frac{1}{w_n \nu_n}\left(\frac{R}{r}\right)^{n+1} T_n = TC_{rr} - V_{rr}$$

where

(13) $$TC_{rr} = \frac{R}{r^2}\sum_{n=2}^{\infty}\left(\frac{-A_{C_0}}{4\pi k}\delta_{n0} + 2\pi\nu_n(\mu H)_n\right)\frac{1}{w_n\nu_n},$$

TC_{rr} is, in fact, the Bouguer correction to the SGD.

The Laplace harmonics of any function like the Moho depth is (Heiskanen and Moritz 1967, p. 30):

(14) $$T_n = \frac{2n+1}{4\pi}\iint_{\sigma} T' P_n(\cos\psi) d\sigma.$$

By substituting Eq. (14) into Eq. (12) and considering Eq. (7) we obtain the following integral equations:

(15) $$\frac{-kR}{r^2}\iint_{\sigma} K(s,\psi) T' d\sigma = TC_{rr} - V_{rr}$$

where the kernel of this integral is:

(16) $$K(s,\psi) = \sum_{n=2}^{\infty}\frac{(n+1)^2(n+2)}{(n-1)} s^{n+1} P_n(\cos\psi),$$

and $s = R/r$.

The kernel (16) is in the spectral form and its generation to infinity is not possible even truncating it to high degree is not economical due to the time consuming generation of the Legendre polynomials. Note that the derived kernel is absolutely convergent as long as $s < 1$, therefore, a closed form formula can be derived for it. To do so, let us write the kernel in the following form:

(17) $$K(s,\psi) = \sum_{n=2}^{\infty}\left(n^2 + 5n + 10 + \frac{12}{n-1}\right) s^{n+1} P_n(\cos\psi).$$

Based on the well-known formula of the Legendre expansion of a reciprocal distance $\frac{1}{l}$ between two points (Heiskanen and Moritz 1967, p. 35):

(18) $$\frac{1}{l} = \sum_{n=0}^{\infty} s^n P_n(\cos\psi),$$

it is not difficult to show that:

(19) $$\sum_{n=2}^{\infty} s^{n+1} P_n(\cos\psi) = \frac{s}{l} - s - s^2\cos\psi$$

(20) $$\sum_{n=2}^{\infty} n s^{n+1} P_n(\cos\psi) = s^2\frac{\partial l^{-1}}{\partial s} - s^2\cos\psi$$

$$= \frac{s^2(\cos\psi - s)}{l^3} - s^2\cos\psi$$

(21)
$$\sum_{n=2}^{\infty} n^2 s^{n+1} P_n(\cos\psi) = s^2\frac{\partial}{\partial s}\left(s\frac{\partial l^{-1}}{\partial s}\right) - s^2\cos\psi =$$
$$= \frac{s^2(s+\cos\psi)}{l^3} - 3\frac{s^3(s-\cos\psi)^2}{l^2} - s^2\cos\psi$$

On the other hand, from Martinec (2003) we already have:

(22) $$\sum_{n=2}^{\infty}\frac{s^{n+1}}{n-1} P_n(\cos\psi) = -s^2\cos\psi + s - sl - s^2\cos\psi\ln\left(\frac{l+1-s\cos\psi}{2}\right)$$

Substitution of Eqs. (19)-(22) into Eq. (17) and simplification of the result yields:

(23) $$K(s,\psi) = \frac{s^2}{l^3}(6\cos\psi - 7s) - \frac{15s^3(s-\cos\psi)^2}{2l^7} - 28s^2\cos\psi + 2s + s\left(\frac{10}{l} - 12l\right) - 12s^2\cos\psi\ln\left(\frac{l+1-s\cos\psi}{2}\right)$$

2. 3. TWO-STEP APPROACH

The process of upward- and downward continuation of the Bouguer correction can be avoided because the topographic information is already available at the Earth's surface. Only V_{rr} is measured at satellite level and needs to be continued downward to Moho, here and after, we call this residual Moho depth and show it by W. In other words, the Bouguer contribution is computed separately and added to W

for obtaining the Moho depth. According to Eqs. (5) and (11) we can write:

$$T_n - 2\pi\nu_n\left(\mu H\right)_n = W_n = \frac{r^2}{R}\nu_n w_n V_{rr,n} \tag{24}$$

Now, we solve this equation for $V_{rr,n}$ and take the summation from degree 0 to ∞ from both sides:

$$\frac{r^2}{R}\sum_{n=0}^{\infty}\frac{W_n}{\nu_n w_n} = V_{rr}\ . \tag{25}$$

From Eqs. (7) and (11) we have:

$$-\frac{4\pi kr^2}{R}\sum_{n=0}^{\infty}\frac{\left(n+1\right)^2\left(n+2\right)}{\left(n-1\right)\left(2n+1\right)}s^{n+1}W_n = V_{rr}\,. \tag{26}$$

According Eq. (14) it is straightforward to rewrite Eq. (26) in the following integral form:

$$-\frac{kr^2}{R}\iint_{\sigma}\sum_{n=0}^{\infty}\frac{\left(n+1\right)^2\left(n+2\right)}{n-1}s^{n+1}P_n\left(\cos\psi\right)W'd\sigma\,. \tag{27}$$

which is an integral equation with a similar kernel function as the one obtained in the one-step approach but it includes the zero- and first-degree terms. Exclusion of these terms does not influence the obtained W as V_{rr} does not include them and due to the orthogonally of the spherical harmonics the derived W is the same whether or not the kernel include the zero- and first-degree terms. Consequently, the closed form formula presented for the kernel function, Eq. (23), can be safely be used for V_{rr} and we can write:

$$-\frac{kr^2}{R}\iint_{\sigma}K\left(s,\psi\right)W'd\sigma = V_{rr}\ . \tag{28}$$

Having computed W from inversion of the integral equation (28), the Moho depth (T) can be derived by:

$$T = W + BC \quad \text{where} \quad BC = 2\pi\sum_{n=0}^{\infty}\nu_n\left(\mu H\right)_n\,. \tag{29}$$

We call this method two-step approach as in the first step the integral equation (28) should be solved for W and in the second one the Moho is derived by adding BC to W.

2. 4. SOLUTION OF INTEGRAL EQUATIONS

Here, we shortly explain how to solve the integral equations by the Tikhonov regularisation (Tikhonov 1963). The integral equations (15) and (28) should be descritised according to the resolution of the desired Moho depths. This process leads to the following system of equations of Gauss-Markov type:

$$\mathbf{Ax} = \mathbf{L} - \boldsymbol{\varepsilon} \tag{30}$$

where $\mathrm{E}\left\{\boldsymbol{\varepsilon}\boldsymbol{\varepsilon}^{\mathrm{T}}\right\} = \sigma_0^2\mathbf{Q}$, $\mathrm{E}\left\{\boldsymbol{\varepsilon}\right\} = 0$ and $\mathbf{A}$ is the coefficient matrix which its number of rows is equal to total number of data and its columns to that of unknowns, $\mathbf{x}$ and $\mathbf{L}$ are the vectors of unknowns and the data, respectively. E stands for the statistical expectation operator; $\mathbf{Q}$ is the cofactor matrix and σ_0^2 is the *a priori* variance factor. Here, we should mention that $\mathbf{A}$ is the same in both one- and two-step approaches, but $\mathbf{x}$ contains T in the one-step method and W in the second method. Correspondingly, $\mathbf{L}$ will be the r.h.s of the integral (15) which is CT_{rr} - V_{rr} in the first method and only V_{rr} in the second one. In this study, number of V_{rr} and T is equal, therefore $\mathbf{A}$ is a squared matrix and there is no redundancy in the system to estimate variance and error of the solution i.e. we assume that $\mathbf{Q} = \mathbf{I}$ and $\sigma_0^2 = 1$.

Equation (30) is ill-conditioned which means that the determinant of $\mathbf{A}$ is very close to zero, not exactly zero, and when it is placed in the denominator for computing the inverse of $\mathbf{A}$ it amplifies the contribution of the high frequencies, which are contaminated with noise of the data, in the solution. This causes that the solution becomes sensitive to the noise of the data. The Tikhonov regularisation is one of the well-known methods for stabilising such a system and it is derived based on minimising the following objective function:

$$\min\left\{\left\|\mathbf{Ax}-\mathbf{L}\right\|_2 + \alpha^2\left\|\mathbf{x}\right\|_2\right\} \tag{31}$$

where α^2 is a positive value which is so-called the regularisation parameter and finally $\left\|\bullet\right\|_2$ stands for the L_2-norm. Solution of Eq. (24) for $\mathbf{x}$ leads to:

$$\mathbf{x}_{\mathrm{reg}} = \left(\mathbf{A}^{\mathrm{T}}\mathbf{A} + \alpha^2\mathbf{I}\right)^{-1}\mathbf{A}^{\mathrm{T}}\mathbf{L} \tag{32}$$

where $\mathbf{x}_{\mathrm{reg}}$ is the regularised solution excluding the erroneous high frequencies. The main issue is to estimate a proper value for α^2. There are different methods to do so, for more details see Hansen (1998). For a short overview on the regularisation methods and their application in inversion of the SGD data see Eshagh (2011a).

2. 5. NUMERICAL STUDIES

In the first part of our numerical studies, the behaviour of the kernel function (23) is presented, after that the meaningfulness of the use of the SGD is investigated. Finally, Iran is selected as the test area

for the determination of Moho depth from the SGD data and testing the feasibility and successfulness of the presented one- and two-step approaches. The last part of the numerical study is dedicated to the practical comparison of these two methods.

2. 5. 1. KERNEL BEHAVIOUR

Equation (23) is the closed form expression of the kernel function (16) and now, we plot it in different geocentric angles ψ to find out if it is a well-behaving kernel and suitable for integral inversion or not. Eshagh (2011b) defined a well-behaving kernel as the one having its highest value at computation point and decays fast to zero. Figure 1 shows the kernel (23) to a geocentric angle of 10°. According to Eshagh's (2011b) definition it is a well-behaving kernel and the inversion of the integral formulae (15) and (29) should be successful. However, the unwanted and unavoidable issue for the integral inversion is the effect of spatial truncation error (STE) which is reducible if the results in the marginal areas are ignored. Eshagh (2011b) stated that the same coverage area for the SGD and unknowns should be considered to reduce the STE. By selecting the results located in the central part this area the distorted unknowns by the STE in the marginal areas are disregarded. The questions is how smaller the central area should be than the whole area? This can be found by plotting the kernel function at different geocentric angles. As Figure 1 shows the kernel value is close to zero after the geocentric angles larger than 6° meaning that the central area should be smaller by 6° than the inversion area.

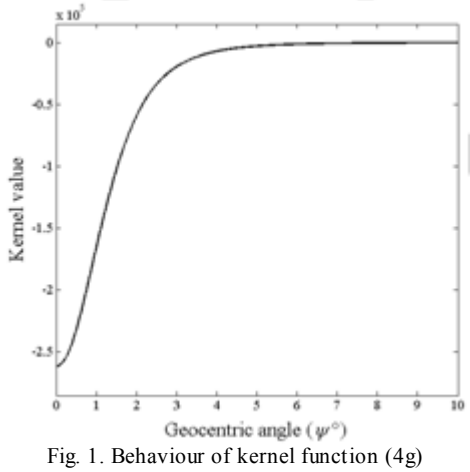

Fig. 1. Behaviour of kernel function (4g)

2. 5. 2. USE OF SATELLITE GRADIOMETRIC DATA: MEANINGFUL OR MEANINGLESS?

Theoretically, we could connect the SGD to the Moho depths by the two presented methods. However, the Moho surface is rather smooth and one cannot expect many fluctuations for it. Is it meaningful to compute the Moho surface by its spherical harmonic expansion to very high degrees? The answer is definitely negative, but what should be the truncation degree? In order to answer this question considers the ratio of the Moho signal after a specific degree of p to total signal.

$$\sqrt{\sum_{n=p}^{N} c_n \Big/ \sum_{n=0}^{N} c_n} \times 100 \le c \qquad (33)$$

where $c_n = \sum_{m=-n}^{n} T_{nm}^2$ and

$$T_{nm} = -\frac{A_{C0}}{4\pi k}\delta_{n0} + 2\pi v_n (\mu H)_{nm} - v_n \Delta g_{nm}$$

where T_{nm}, $(\mu H)_{nm}$ and Δg_{nm} are the spherical harmonic coefficients of Moho depths, product of topographic masses and heights and free-air gravity anomaly, respectively.

The plot of the ratio (7) should be decreasing with the increase of p towards N which is highest truncation degree but not the optimum one. Here, EGM08 (Pavlis et al. 2008) to degree and order 360 is considered to generate c_n as the Moho model does not include higher degrees at least the one derived from the SGD. The ratio (7) is plotted in Figure 2 when p ranges from 0 to 360. Depending on the value of c different truncation degrees can be found. Assuming c = 1% means that the percentage of the Moho signal after degree 215 is less than 1% and similarly for c = 0.1% it will be 357. Consequently, the use of SGD is useful and meaningful as they are sensitive to frequencies corresponding to degree and order 250 in the equivalent spherical harmonic expansion and at least there is no loss of frequency of the Moho model.

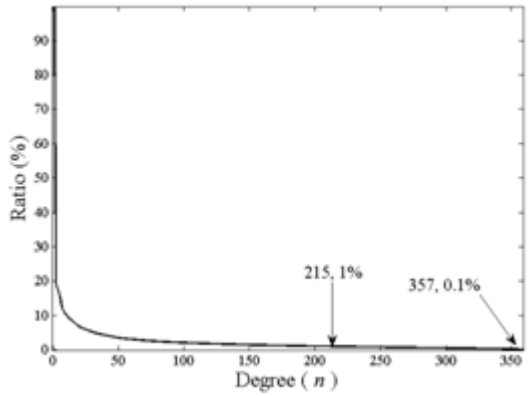

Fig. 2. Ratio of Moho signal at high degrees to total signal

2. 5. 3. NUMERICAL STUDIES IN IRAN

We select an area which is limited between latitudes of 15°N and 50°N and longitudes of 35°E and 75°E so that Iran is placed in its central part to reduce the STE of the integral formulae. Here, we use EGM08 (Pavlis et al. 2008) and the Moho model of CRUST1.0 (Laske et al. 2013) and DTM2006

topographic height model (Pavlis et al. 2006) and all to degree and order 180. Figure 3 shows the maps of the SGD over the study area in unit of E (Eötvös) and illustrates the largest and negative value at Caspian Sea and the positive one over the Zagros Mountains and in the north-east part of Iran around its border to Azerbaijan and Turkey and in the south part in Bam. The SGD have extreme values over these areas compared to those mountains which are continuation of Himalaya Mountains in Afghanistan. Figure 3b is the map of CT_{rr} and its general pattern is very similar to the map of V_{rr} presented in Figure 3a but the largest positive magnitudes is seen in Afghanistan and the negative ones over the Oman Sea and Indian Ocean. Its magnitude is about 10 times larger than the SGD meaning that they have more contribution to the Moho than the SGD.

Figures 3c and 3d are the maps of gravimetric and seismic Moho models in units of km. Two important parameters should be selected prior to computing the gravimetric Moho model:

a) the density contrast between the mantle and crust.
b) the mean Moho depth.

Here, we selected a density contrast of 600 gr/cm^3 and found the mean value of Moho by comparing the generated gravimetric Moho model to the seismic model of CRUST1.0. The best match found when a mean Moho depth of 35 km is considered for generating the gravimetric Moho model so that the root mean squared error (RMS) between the models became 8.7 km. The RMS 8.7 km seems to be very large but if we look at Figures 3c and 3d we can see that these two models are very different.

Table 1 shows the statistics of V_{rr}, CT_{rr}, gravimetric and seismic Moho models. V_{rr} ranges from -1.1 E to 0.9 E over the area and CT_{rr} is rather large and reach to a maximum value of 5.0 E. The maxima of both Moho models are close but their minima differ considerably by about 18 km. The standard deviation (STD) of the gravimetric model is smaller than the seismic one which can be somehow interpreted as its smoothness. The mean value of the seismic model is very close to 35 km but that of the gravimetric model is larger by 2.5 km. This is due to the fact that 35 km is a global mean value and it does not warrant being the same in a local area like Iran.

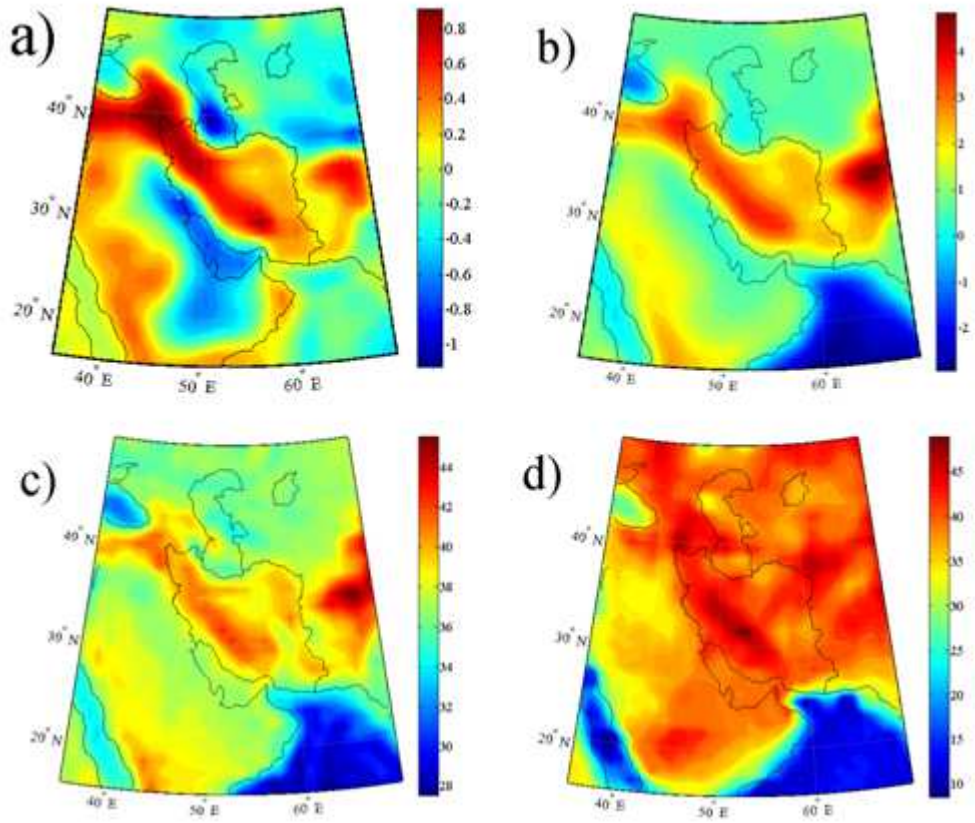

Fig. 3. a) V_{rr} *at* 250 km level [E], b) CT_{rr} at 250 km level [E], c) gravimetric Moho model [km] and d) seismic Moho model of CRUST 1.0 [km].

Table 1. Statistics of V_{rr}, CT_{rr} and gravimetric and seismic Moho models

	Max	Mean	Min	STD
V_{rr} [E]	0.9	0.0	-1.1	0.4
CT_{rr} [E]	5.0	1.1	-2.9	1.4
Gravimetric Moho [km]	47.7	37.5	26.3	3.4
Seismic Moho [km]	49.6	35.6	8.5	9.3

2. 5. 3. 1. NUMERICAL STUDY ON ONE-STEP APPROACH

Now, the integral equation (15) is used to recover the Moho depths directly from CT_{rr}. In this method CT_{rr} is added to V_{rr}. Since the organised system of equations after discretisation of the integral formula is ill-conditioned and sensitive to the error of V_{rr}, the solution is stabilised to get meaningful results by the Tikhonov Regularisation method. Regularisation Tools of MATLAB (Hansen 2007) is applied to solve this system of equations with combination with L-curve method for estimating the regularisation parameter. The same coverage is considered for both of T and V_{rr}. Two resolutions of $1^\circ \times 1^\circ$ and $0.5^\circ \times 0.5^\circ$ are considered for recovering T and for reducing the effect of the STE, the results in the central area which is smaller by 1°, 2°, …, 8°, than the inversion area are selected.

Figure 4a shows the recovered T based on the one-step approach with a resolution of $1^\circ \times 1^\circ$ in a central area smaller than the whole area by 6°. Figure 4b is a similar map of the Moho model but with a resolution of $0.5^\circ \times 0.5^\circ$. Both of them have similar patterns but Figure 4a is smoother than Figure 4b due to the lower resolution. One issue that should be explained here is observing positive and negative values for T. The reason is that recovering all frequencies of the Moho signal is not possible by the one-step approach as the zero- and first-degree harmonics have been already removed from the kernel. Recovering a global value for the mean Moho depth using local data and a kernel which is inherently blind to the first-degree is not possible. Therefore, the depths which are recovered from inversion of integral (15) do not contain the zero- and first-degree harmonics. If we restore these degrees on the recovered to T the map presented in Figure 4c is derived.

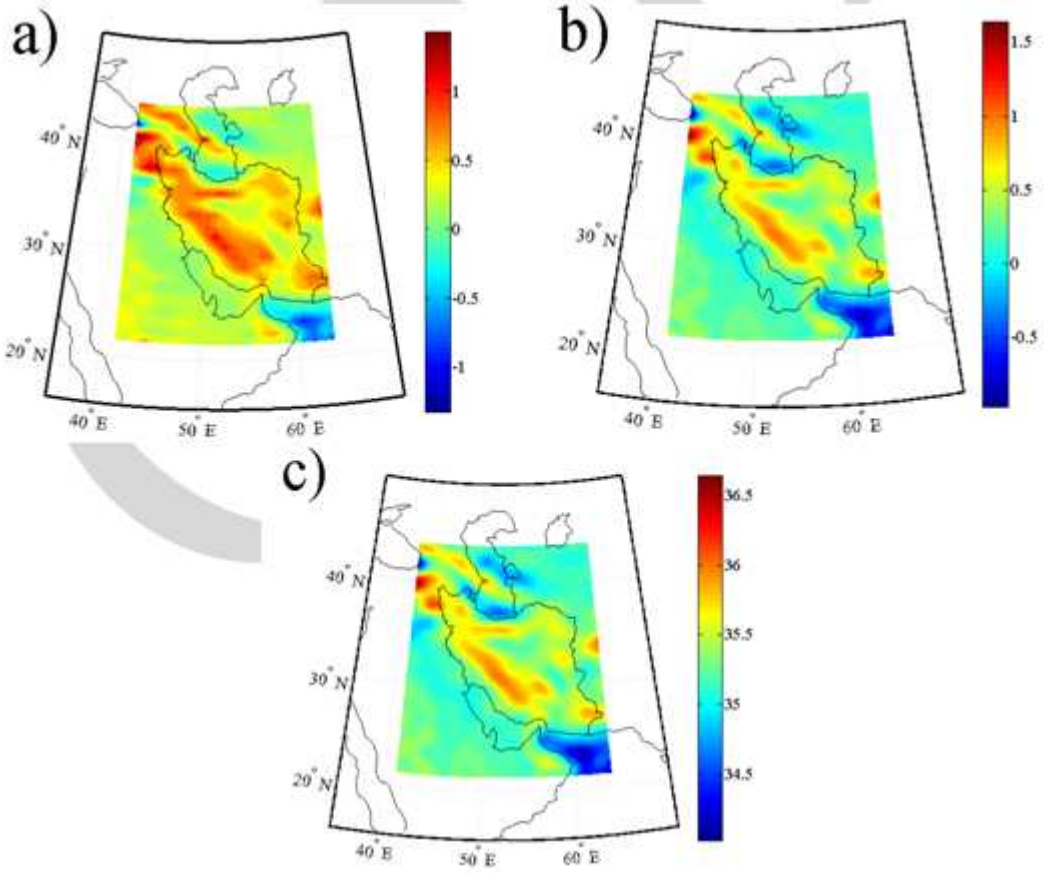

Fig. 4. Recovered Moho depths excluding the contribution of zero- and first-degree harmonics with a resolution of a) $1^\circ \times 1^\circ$ and b) $0.5^\circ \times 0.5^\circ$ and c) Moho depths after restoring zero- and first-degree harmonics. Unit: 1 km

In order to evaluate the quality of the inversion, the Moho model computed by EGM08 and Eq. (4) and (5) is compared to the one recovered from V_{rr} in different resolutions and sizes of the central area. The statistics of the differences between these models are presented in Table 2. One could see in the table that the extreme values are reduced by reducing the size of central area, but in the opposite, the mean value of the differences increases. The reason is that the system of equations is solved for whole area based on Tikhonov regularisation and the Moho undulations are obtained around the estimated mean value of the whole area and not the central one. Therefore, by reducing the size of this area the mean value changes from that of the whole area. The reduction of the extreme values leads to decrease of the STDs. However, judging about the quality by STD is not fully correct as when the solution is smooth the STD becomes small as well. The RMS value decreases but remains constant by reducing the size of central area because when STD reduces the mean value increases therefore it remains with the same value, but after 6° it starts growing up which is not desired. One can conclude that the central area should be 6° smaller than the whole area. In the last column of the table the correlation between both models is presented in the selected central areas and it shows that when the resolution of the unknowns is $0.5^\circ \times 0.5^\circ$ the correlation is higher.

A correlation of higher than 90% is seen when the central area is 6° smaller than the inversion area. Moreover, the table shows that the resolution of the unknowns does not play an important role in the results, also as Figure 4c shows, more detailed information can be achieved but the magnitudes of the depths do not change. Figure 4c is the map of the Moho depths after restoring the zero- and first-degree harmonics to the recovered Moho depths. The maximum, mean, minimum and STD of this model are 36.7, 35.3, 34.0 and 0.3 in unit of km, respectively.

Table 2. Statistics of differences between Moho models computed from EGM08 and one-step approach from V_{rr}. Unit: 1 km

Resolution	Central area smaller by	Max	Mean	Min	STD	RMS	corr
$1^\circ \times 1^\circ$	1°	9.5	-2.2	-11.7	3.0	3.7	64.2%
	2°	8.1	-2.3	-11.3	2.8	3.6	78.5%
	3°	7.6	-2.5	-11.1	2.6	3.6	82.0%
	4°	7.1	-2.6	-9.6	2.5	3.6	85.3%
	5°	6.9	-2.7	-9.1	2.3	3.6	86.0%
	6°	6.9	-2.9	-8.3	2.2	3.6	88.6%
	7°	6.3	-3.0	-8.3	2.1	3.7	90.1%
	8°	5.7	-3.2	-8.3	2.0	3.8	91.9%
$0.5^\circ \times 0.5^\circ$	1°	9.5	-2.2	-11.5	3.0	3.7	76.5%
	2°	8.2	-2.3	-11.5	2.8	3.6	87.8%
	3°	8.2	-2.5	-11.5	2.6	3.6	88.7%
	4°	7.6	-2.6	-10.0	2.5	3.6	90.2%
	5°	6.9	-2.7	-9.7	2.3	3.6	90.7%
	6°	6.9	-2.9	-8.4	2.2	3.6	92.1%
	7°	6.5	-3.0	-8.4	2.1	3.7	93.3%
	8°	5.8	-3.2	-8.4	2.0	3.8	94.1%

2. 5. 3. 2. NUMERICAL STUDY ON TWO-STEP APPROACH

The Moho model delivered by the one-step method is very smooth and has STD and RMS values of 2.2 km and 3.7 km, respectively. Nevertheless, as already mentioned *BC* is computed at sea level and does not need to be continued upward and downward, otherwise extra errors due to solving the ill-conditioned integral equations occurs for the *BC* too. However, the two-step approach avoids such a process and only inverts the SGD to *W* instead of *T*.

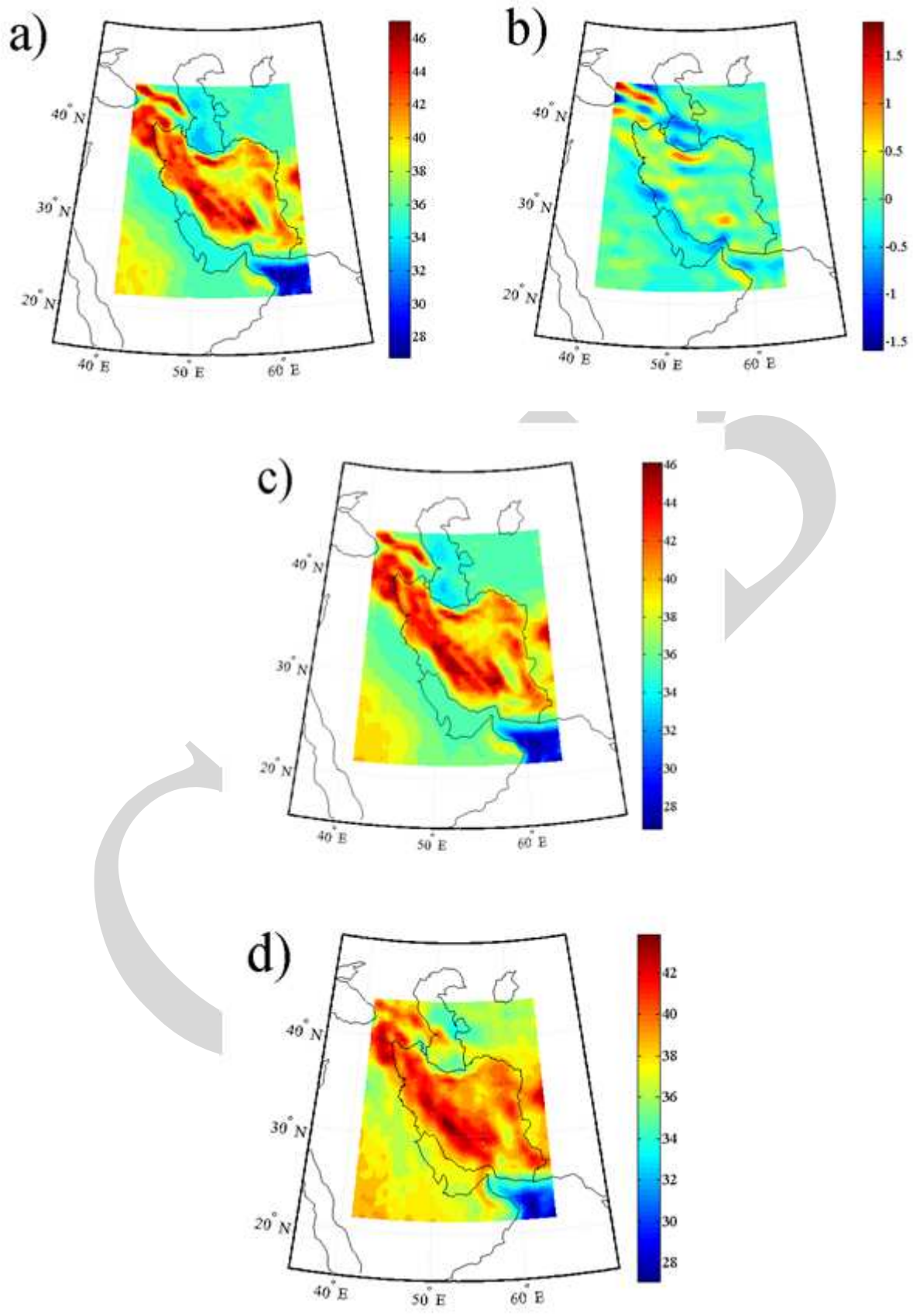

Fig. 5. a) *BC*, b) *W*, c) Moho depths by two-step approach, d) Moho depths derived from EGM08. Unit: 1 km

Figure 5a is the map of *BC*. In comparison with Figure 2c which is the gravimetric Moho model of the area, one can see that *BC* is about 10 times larger than *W*. Figure 2d shows that *W* contributes about 2 km to *T*. When *W* is added to *BC*, *T* is derived and presented in Figure 5c. Figure 5d is the Moho model which directly computed by Eq. (1) and EGM08. Figures 5c and 5d are theoretically the same Moho model but derived from different data. Figure 5c shows more detailed model than Figure 5d. The derived model from the SGD is deeper in Bam and Damavand. Also Urmia Lack is more visible in Figure 5c than Figure 5d. Figure 5d shows that there is a deep Moho in the western part of Caspian Sea which does not seem to be true whilst Figure 5c does not show such a depth in that area.

In order to do a better comparison, the statistics of the Moho models and their differences are presented in Table 3.

Table 3. Statistics of *W*, *BC* and Moho depths recovered from SGD and EGM08 and their differences. Unit: 1 km.

	Max	Mean	Min	STD	RMS
W	1.6	0.0	-2.0	0.3	-
BC	48.1	38.2	26.8	3.5	-
SGD Moho	47.1	38.2	26.8	3.3	-
EGM08 Moho	44.3	38.0	27.1	2.5	-
BC – EGM08 Moho	6.3	0.2	-5.4	1.7	1.7
SGD Moho – EGM08 Moho	5.3	0.2	-4.8	1.5	1.5

It represents that *W* ranges from -2 km to 1.6 km with a zero mean value and STD of 300 m. The term related to *BC* is quite large and reaches to 48.1 km and the mean value of 38.2 km. By adding *W* to this term the mean value and the minimum value of Moho depths do not change but the maximum value reduces to 47.1 km. The reason of this reduction is that *W* has the opposite sign to *BC*. The Moho model recovered from EGM08 ranges from 27.1 km to 44.3 km with mean value and STD of 38 km and 2.5 km. The small STD can be, somehow, interpreted as the smoothness of this Moho model with respect to the one recovered from V_{rr}.

Also this can be due to the fact that *W* is smaller in magnitude than the gravity anomalies obtained from EGM08. The last two rows of the table represent the statistics of the differences between *BC* and EGM08 Moho model as well as *T* and EGM08 Moho. The RMS of these differences is 1.7 km and the RMS of the differences between the Moho of V_{rr} and EGM08 is 1.5 km showing that *W* is in order of the difference between *BC* and EGM08 Moho can very well present them. It should be stated that EGM08 has been used to degree and order 360 and we already know that V_{rr} do not sense the gravity field to these degree. However, they could cover majority of the signal.

2. 5. 4. ONE-STEP OR TWO-STEP APPROACH?

According to the presented numerical studies in the last two sections, it is straightforward to conclude that the two-step approach performs better. The reason is that only V_{rr} is inverted whilst the one-step approach inverts both of V_{rr} and CT_{rr}. Although the kernel function of both methods is the same but since the system of equations is ill-conditioned the solution will be very sensitive to that r.h.s. the system. When it is a smoother quantity the inversion process is more successful. Another issue is the smoothing property of the used regularisation technique, i.e. Tikhonov Regularisation. In fact, any regularisation method delivers a smooth solution by cutting the higher frequencies. Now, if the r.h.s of the system of equations is large in magnitude the contribution of its high frequencies is also large and vice versa.

In our numerical studies we showed that *BC* is much larger than *W* and it is obvious that in the regularisation process higher frequencies of this part are very large and when they are removed from them solution large part of the signal is neglected. But when we use only V_{rr} at 250 km level, the data is smooth and small portion of them is cut during the inversion process. Moreover, the contribution of the first- and second-degree harmonics of the Moho should be removed from the data and restored to the results afterwards, but in the case of using the two-step method is process is done inherently by adding *BC* and since the kernel of the integral does not include the zero- and first-degree terms it will filter out the corresponding frequencies from V_{rr} even if V_{rr} includes them. Therefore, the Moho recovery process by the two-step method is more successful than the one-step one.

3. RESULTS AND DISCUSSION

Amongst few studies about Moho recovery from the SGD data we can mention the works done by Reguzzoni and Sampietro (2012), Reguzzoni et al. (2013) and Barzaghi et al. (2013), but the present work uses a similar idea to that used by Bagherbandi and Eshagh (2011,2012). In both of the studies, the VMM theory is used. However, Bagherbandi and Eshagh (2011, 2012) used the isostatic equation of equilibrium for the second-order derivative of the disturbing potential. They derived nonlinear integral equations and solved it numerically.

One problem of that work is the requirement of approximate values of the Moho depths for the

computation of them they used the spherical harmonic series presented in Eq. (1). Consequently, the main goal was to obtain higher frequencies of the Moho variations from the SGD and add them to the approximate model. Their system of equations, organised after lineraisation of the integral equation, was difficult to solve as they had to invert an integral with a specific kernel function but for updating the SGD from the recovered Moho model they had to use another integral with a different kernel, which was quite time consuming. Furthermore, the STEs of both forward and inverse problems were not the same.

On the other hand, their numerical studies showed that the Moho model cannot be recovered with higher resolution than $2^\circ \times 2^\circ$ as the system of equations became very unstable and difficult to stabilise, whilst our method is capable to do the recovery to a resolution of $0.5^\circ \times 0.5^\circ$. One issue that should be explained here is whether or not these complicated processes are meaningful. If we look at Eq. (3), we observe that the Moho depth formula has three terms which are all functions of the approximate Moho depth (*T*).

It is obvious that the second and third terms of this formula are just some improvements to *T*. However, in the case of using SGD we cannot expect to reach to them due to the satellite elevation and smooth nature of the Moho surface. Bagherbandi (personal communication) stated that the contribution of the third term is smaller than the second term too. It could be expected as the numerator of the integrant is the difference between the Moho depths at the computation and integration points and since Moho is smooth this difference cannot be large. Now according to the seismic Moho model of CRUST1.0 presented in Figure 2d we can see that the maximum depth of Moho reaches to 46 km in Iran.

Therefore, it will not be difficult to see how large the approximation of Eq. (3) to the first term will be. If assume that R = 6400 km the magnitude of the second term is at most $46^2/6400$=0.3 km which is negligible comparing to the size of Moho depths. Therefore, it is reasonable to compute the Moho model only by the first term as the mathematical models becomes very simple and the integral equation for inverting the SGD becomes linear. After solving it for the depths the effect of the second and third terms are considered.

4. CONCLUSIONS

We presented a simple linear integral equation for recovering Moho model from satellite gradiometry data (SGD). Also, we showed that approximating the Moho determination formula based, on the Vening Meinesz-Moritz theory presented in Eq. (3), to the first term commits only 300 m error in Iran which is very small comparing to the magnitude of the Moho depth.

Since the Moho surface is smooth recovering its short wavelengths is not very meaningful especially from SGD data. In this study, by the use of EGM08 to degree and order 360 we found out that the contribution of higher degree harmonics than 215 is less than 1%, which is high enough to justify the use of the SGD and the presented theory because other type of satellite data are not as sensitive as the SGD. Two methods of one-step and two-step were presented for the Moho recovery goal and our numerical studies showed that the first method delivers an over-smoothed model whilst the second method is more successful.

It can deliver the Moho model with a root mean squared error of 1.5 km with respect to the Moho model of EGM08 which is quite good and it presents more detailed information about the Moho depths than the one-step method. Here, we recommend using the two-step method for the Moho recovery from SGD but emphasise that the Bouguer contribution should not be continued upward to the SGD as they should be continued downward again.

ACKNOWLEDGMENT

The author is thankful to Professor Lars E. Sjöberg at Royal Institute of Technology (KTH), Stockholm and Docent Mohammad Bagherbandi at University of Gävle, Sweden for the stimulating discussions about the subject. The Swedish National Space Board (SNSB) is acknowledged for the financial support of Project 116/12.

REFERENCES

Airy, G.B. (1855) On the computations of the effect of the attraction of the mountain masses as disturbing the apparent astronomical latitude of stations in geodetic surveys. *Trans. Royal Society* (London), Series B, 145, 1855.

Bagherbandi, M. & Eshagh, M., (2011) Recovery of Moho's undulations based on the Vening Meinesz-Moritz theory from satellite gravity gradiometry data: A simulation study, Advances in Space Research, 49 (6), 1097-1111.

Bagherbandi, M. & Eshagh, M. (2012) Crustal Thickness Recovery Using an Isostatic Model and GOCE Data. *Earth, Planets and Space (EPS)*, 64 (11), 1053-1057.

Bagherbandi, M. & Sjöberg, L.E. (2011) Comparison of crustal thickness from two isostatic models versus CRUST2.0. *Studia Geophysica Et Geodaetica*, 55, 641-666.

Barzaghi, R., Reguzzoni, M., Borghi A., De Gaetani C., Sampietro D. & Marotta A.M. (2013) *Global to local Moho estimate based on GOCE Geopotential Model and Local Gravity Data*. Proceedings of IAG 2013 Symposium.

Bassin, C., Laske, G. & Masters, T.G. (2000) The current limits of resolution for surface wave tomography in North America. *Eos, Transactions American Geophysical Union*, 81, F897.

Braitenberg, C., Zadro, M., Fang, J., Wang, Y. & Hsu, H.T., (2000) The Gravity and Isostatic Moho Undulations in Qinghai-Tibet Plateau. *Journal of Geodynamics*, 30 (5), 489-505.

Braitenberg, C., Wienecke, S. & Wang, Y. (2006) Basement structures from satellite-derived gravity field: South China Sea ridge. *Journal of Geodynamics Research*, 111, B05407, doi:10.1029/2005JB003938.

Braitenberg, C. & Ebbing, J. (2009) New Insights Into the Basement Structure of the West-Siberian Basin From Forward and Inverse Modelling of Grace Satellite Gravity Data. *Journal of Geophysical Research*, 114, B06402.

Čadak, O. & Martinec, Z. (1991) Spherical Harmonic Expansion of the Earth's Crustal Thickness Up to Degree and Order 30. *Studia Geophysica Et Geodaetica*, 35, 151-165.

Gomez-oritz, D. & Agarwal, B.N.P. (2005) 3D INVER.M: a MATLAB Program to Invert the Gravity Anomaly over A 3D Horizontal Density Interface by Parker-Oldenburg's Algorithm. *Computers & Geosciences*, 31: 13-520.

Kiamehr R. & Gomes-Ortiz D., 2009, A New 3D Moho Depth Model for Iran Based on the Terrestrial Gravity Data and EGM2008 Model. *European Geosciences Union (EGU) General Assembly*, 11, EGU2009-321-1, Vienna, Austria (Abstract).

Eshagh, M. (2009a) On Satellite Gravity Gradiometry, Doctoral Dissertation in Geodesy, Royal Institute of Technology (KTH), Stockholm, Sweden.

Eshagh, M. (2009b) The Effect of Lateral Density Variations of Crustal and Topographic Masses on GOCE Gradiometric Data: A Study In Iran And Fennoscandia. *Acta Geodaetica et Geophysica Hungarica*, 44 (4), 399-418.

Eshagh, M. (2010) Comparison of Two Methods of Considering Laterally Varying Density in Topographic Effect on Satellite Gradiometric Data. *Acta Geophysica*, 58 (4), 661-686.

Eshagh, M. (2011a) Sequential Tikhonov Regularization: An Alternative Way for Integral Inversion of Satellite Gradiometric Data. *Zeitschrift fur Geodasie, Geoinformation und Landmanagement (ZfV)*, 136, 113-121.

Eshagh, M. (2011b) The effect of spatial truncation error on integral inversion of satellite gravity gradiometry data. *Advances in Space Research*, 47, 1238-1247.

Eshagh, M. (2011c) Inversion of satellite gradiometry data using statistically modified integral formulas for local gravity field recovery. *Advances in Space Research*, 47 (1), 74-85.

Eshagh, M. & Bagherbandi, M. (2012) Quality Description for Gravimetric and Seismic Moho Models of Fennoscandia Through a Combined Adjustment. *Acta Geodaetica Et Geophysica Hungarica*, 47 (4), 388-401.

Eshagh, M. & Sjöberg, L.E. (2011) Determination of Gravity Anomaly at Sea Level from Inversion of Satellite Gravity Gradiometric Data. *Journal of Geodynamics*, 51, 366-377.

Eshagh, M., Bagherbandi, M. & Sjöberg, L.E. (2011) A Combined Global Moho Model Based On Seismic And Gravimetric Data. *Acta Geodaetica et Geophysica Hungarica*, 46, 25-38.

Hansen, P.C. (1998) *Rank-Deficient and Discrete Ill-Posed Problems: Numerical Aspects of Linear Inversion*. SIAM, Philadelphia.

Hansen, P.C. (2007) Regularization Tools version 4.0 for Matlab 7.3. *Numerical Algorithms*, 46, 189-194.

Heiskanen, W.A. (1931) *New Isostatic Tables for the Reduction of the Gravity Values Calculated on the Basis of Airy's Hypothesis. Publication of the Isostatic Institute of the Internat. Association of Geodesy (Helsinki)*, 2.

Heiskanen, W. & Moritz, H., 1967, *Physical geodesy*, W.H. Freeman and Company, San Francisco and London.

Janak, J., Fukuda, Y. and Xu, P. (2009) Application of GOCE Data For Regional Gravity Field Modeling, Earth. *Planets and Space (EPS)*, 61, 835-843.

Laske, G., Masters, G., Ma, Z. and Pasyanos, M. (2013) *Update on CRUST1.0 - A 1-degree Global Model of Earth's Crust*. In EGU General Assembly Conference Abstracts 15: 2658.

Martinec, Z. (1993) A Model of Compensation of Topographic Masses. *Survey in Geophysics*, 14 (4-5), 525-535.

Martinec, Z. (1994) The density contrast at the Mohorovičič Discontinuity. *Geophysical Journal International*, 117, 539-544 .

Martinec, Z. (2003) Green's Function Solution To Spherical Gradiometric Boundary-Value Problems. *Journal of Geodynamics*, 77, 41-49.

Moritz, H. (1990) *The Figure of the Earth*, H Wichmann, Karlsruhe.

Oldenburg, D.W. (1974) The Inversion and Interpretation of Gravity Anomalies. *Geophysics*, 39, 526-536.

Pavlis, N., Factor, K. & Holmes, S.A. (2006) *Terrain-Related Gravimetric Quantities Computed for the Next EGM*. Presented at the 1st International symposium of the International gravity service 2006, August 28- September 1, Istanbul, Turkey.

Pavlis, N., Holmes, S.A., Kenyon, S.C. & Factor, J.K. (2008) *An Earth Gravitational model to degree 2160: EGM08*. Presented at the 2008 General Assembly of the European Geosciences Union, Vienna, Austria, April 13-18, 2008.

Parker, R.L. (1972) The rapid calculation of potential anomalies. *Journal of Geophysical Research: Atmospheres*, 31, 447-455.

Reed, G.B. (1973) *Application of Kinematical Geodesy For Determining The Shorts Wavelength Component of The Gravity Field By Satellite Gradiometry*, Ohio State

University, Department of Geode Science, Representative No. 201, Columbus, Ohio.

Sampietro, D. (2009) *An Inverse Gravimetric Problem With GOCE Data*. Ph.D. thesis. Politecnico di Milano Polo regionale di Como. 2009.

Sampeitro, D. (2011) *GOCE exploitation for Moho modelling and applications*. In proceedings of the 4th international GOCE user workshop, Munich, Germany, Vol: 31.

Sampietro, D. & Reguzzoni, M. (2011) *A Study on the Austrian Moho from GOCE Data.* Poster presented at European Geosciences Union General Assembly 2011 Vienna, Austria, 08 April 2011.

Reguzzoni, M. & Sampietro, D. (2012) *A New Global Crustal Model Based on GOCE Data Grids*. Presented at First International GOCE Solid Earth Workshop, Enschede, The Netherlands

Regizzoni, M. Sampietro, D. & Sanso, F. (2013) Global Moho from the Combination of the CRUST2.0 model and GOCE data. *Geophysical Journal International*, 195 (1), 222-237

Shin, Y.H., Xu, H., Braitenberg, C., Fang, J. & Wang, Y. (2007) Moho undulations beneath Tibet from GRACE-integrated gravity data. *Geophysical Journal International*, 170, 971-985.

Sjöberg, L.E. (2009) Solving Vening Meinesz-Moritz Inverse Problem in Isostasy. *Geophysical Journal International*, 179, 1527-1536.

Sjöberg, L.E. & Bagherbandi, M. (2011) A Method of Estimating the Moho Density Contrast with a Tentative Application by EGM08 and CRUST2.0. *Acta Geophysica*, 58, 1-24.

Sünkel, H. (1985) *An Isostatic Earth Model*, Report 367, Department of Geodetic Science and Surveying, Ohio State University, Columbus. Ohio.

Tapley, B., Ries, J. Bettadpur, S., Chambers, D., Cheng, M., Condi, F., Gunter, B., Kang, Z., Nagel, P., Pastor, R., Pekker, T., Poole, S. & Wang, F. (2005) GGM02-An Improved Earth Gravity Field Model From GRACE. *Journal of Geodynamics*, 79, 467-478

Tenzer, R., Hamayun & Novak, P. and Vajda, P. (2009) Global Maps Of The CRUST2.0 Components Stripped Gravity Disturbances. *Journal of Geophysical Research (Solid Earth)*, 114, B05408.

Tenzer, R., Hamayun Novak ,P., Gladkikh, V. & Vajda P., 2012, Global crust-mantle density contrast estimated from EGM08, DTM2008, CRUST2.0 and ICE-5G. *Pure and Applied Geophysics*, 169 (9), 1663-1678.

Tikhonov, A.N. (1963) *Solution of Incorrectly Formulated Problems And Regularization Method*. Soviet Math. Dokl., 4: 1035-1038. English translation of Dokl. Akad. Nauk. SSSR, 151, 501-504.

Vening Meinesz, F.A. (1931) Une nouvelle methode pour la reduction isostatique regionale de l'intensite de la pesanteur. *Bulletin Géodésique*, 29, 33-51.

Xu, P. (1992) Determination of surface gravity anomalies using gradiometric observables. *Geophysical Journal International*, 110, 321-332.

Xu, P. (1998) Truncated SVD methods for discrete linear ill-posed problems. *Geophysical Journal International*, 135, 505-514.

Xu, P. (2009) Iterative generalized cross-validation for fusing heteroscedastic data of inverse ill-posed problems. *Geophysical Journal International*, 179, 182-200.